Available online at www.sciencedirect.com
ScienceDirect
Mendeleev Commun., 2015, **25**, 299–301
Mendeleev Communications

Ultraviolet luminescence of commercial cerium-doped yttrium aluminum garnet phosphors

Anatoly V. Vishnyakov,*[a] Ekaterina A. Vishnyakova,[b] Tatiana Yu. Kiseleva[c] and Ivan V. Ivanov[a]

[a] *D. I. Mendeleev University of Chemical Technology of Russia, 125047 Moscow, Russian Federation. Fax: +7 499 978 5991; e-mail: prof_vav@mail.ru*
[b] *International Laser Center, M. V. Lomonosov Moscow State University, 119991 Moscow, Russian Federation*
[c] *Department of Physics, M. V. Lomonosov Moscow State University, 119991 Moscow, Russian Federation*

DOI: 10.1016/j.mencom.2015.07.024

The origin of the intense UV luminescence of commercial YAG:Ce phosphors has been established based on the data of X-ray diffraction, optical spectroscopy and scanning electron microscopy.

The luminescence spectra of YAG:Ce-based commercial phosphors prepared by us contain a high-intensity luminescence band in the UV spectral range in addition to a usual yellow-orange band.[1] To interpret the results, we have suggested that the high-intensity UV luminescence peak has an impurity nature. The aim of this work was to elucidate the origin of UV luminescence from these phosphors.

The synthesis of commercial garnet-based phosphors is usually carried out in the presence of mineralizing salts (flux additives) capable of enhancing mass transfer in the reaction mixture. The concentration of these additives is varied from 1.0 to 20%.[2] In order to study the influence of flux additives on UV luminescence three samples were examined: sample 1 of the commercial phosphor was compared to samples 2 and 3 prepared at 1500 °C under the conditions of synthesis described previously.[1] Initial compositions for the synthesis of all samples contained barium chloride and fluoride mixtures. The BaF_2 contents of samples 1 and 2 were 9 and 6 wt%, respectively. The $BaCl_2$ content of all samples was 4 wt%. Sample 3 was obtained by the additional long-term (4 h) calcination of sample 2 at 1580 °C in a flow of $N_2 + H_2$.

The phase composition of the synthesized samples was determined by X-ray diffraction analysis (Figure 1).[†] The main component in all samples was the cubic phase $Y_3Al_5O_{12}$ [98-006-7102] (garnet structural type, space group *Ia*3*d*). The grain sizes of the main crystalline phase were found to increase from sample 1 to sample 3, and they were estimated using the Williamson–Hall method as 0.5, 1.0 and 2.6 μm, respectively.

The XRD pattern of sample 1 [Figure 1(*a*)] contains weak diffraction maxima that show a small amount of the impurity phase $BaCeF_5$ [98-004-0298] (cubic lattice, space group *Fm*–3*mx*). The integral width of the structural maxima of this phase is almost twice as large as that of the main phase, which is indicative of a strong dispersion of the impurity.

For sample 2, the XRD pattern also contains weak diffraction maxima [Figure 1(*b*)] due to the presence of small impurities. One of these phases is reliably identified as BaFCl [98-008-5319] (tetragonal lattice, space group *P*4/*nmm*). Another identified impurity phase (with structural maxima at angles of 25.27°, 29.36° and 42.11°) has a cubic lattice of the $BaCeF_5$ type. A shift of this phase diffraction maxima toward smaller angles (which is the evidence of increased interplanar distance) can be explained by the formation of particles with a structure of the type of dilute solid solution $BaCeF_{5-x}Cl_x$. A difference of the ion radii of Cl (0.181 nm) and F (0.133 nm) does not exceed 30%, which makes their mutual substitution acceptable.

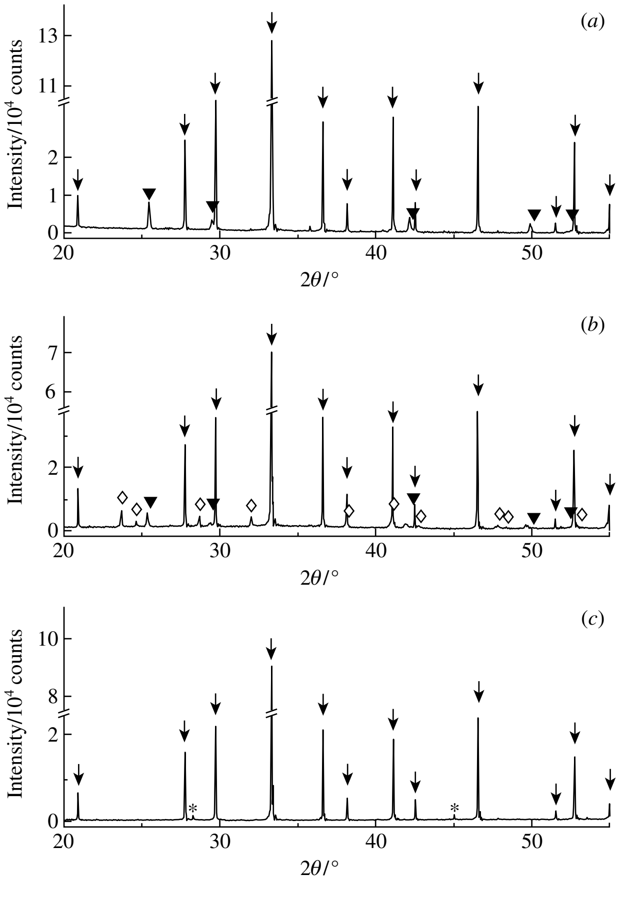

Figure 1 Fragments (magnified) of the XRD patterns of phosphor powders in the region of most pronounced diffraction peaks of impurity phases: (*a*) sample 1, (*b*) sample 2 and (*c*) sample 3. Arrows indicate peaks of the YAG phase, symbols indicate peaks of impurity phases BaFCl (rhombs), $BaCeF_5$ (triangles), and $BaAl_2O_4$ (asterisks).

A small (~2%) impurity phase is Al_2BaO_4 [98-001-6845] with a hexagonal lattice (space group *P*6322) in sample 3 [Figure 1(*c*)].

[†] The powder diffraction data were collected in a scan mode on an Empyrean powder diffractometer (PANalytical Co., Netherlands) equipped with a Pixel3D detector, in Bragg-Brentano geometry (θ–2θ scan) using nickel-filtered CuKα radiation. The XRD patterns were analyzed using the HighScore program package and the JSPDS PDF4 database.

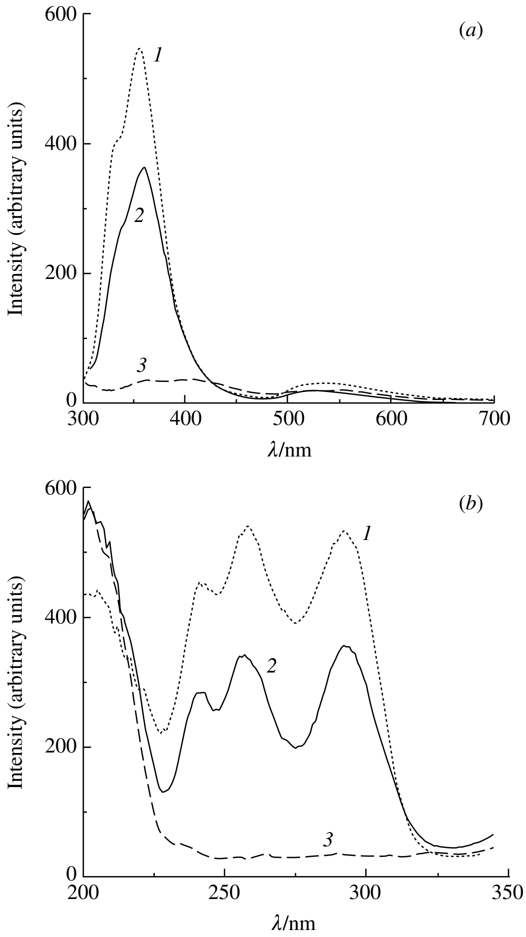

Figure 2 The (*a*) luminescence spectra (excitation wavelength, 294 nm) and (*b*) excitation spectra (detection wavelength, 360 nm): (*1*) sample 1, (*2*) sample 2 and (*3*) sample 3.

Note that, in the X-ray diffraction patterns of samples 1 and 2, there are no reflections belonging to the $BaCl_2$ phase. This effect results from the interaction between barium chloride and barium fluoride at the stage of phosphor synthesis (1500 °C) and the distribution of chloride into a $BaCeF_5$ phase.

Figure 2 shows the luminescence and excitation spectra of suspensions prepared from the synthesized phosphors.[‡] The luminescence spectrum of sample 2 exhibits a set of bands identical to that observed for sample 1, which comprises an intense UV band at ~360 nm and a weak band in the visible range at ~540 nm. The latter peak (near 540 nm) was observed for all the samples and was associated with the yellow luminescence of $Y_3Al_5O_{12}$:Ce phase. The ratio of intensities of the UV luminescence bands for samples 2 and 1 was 1 : 1.5, which pointed to certain correlation with the content of BaF_2.

The excitation spectra of these samples exhibit a superposition of three clearly expressed peaks (~242, ~258 and ~294 nm). The absence of significant differences in the UV luminescence spectra of these samples excited at 292 and 258 nm indicated that these excitation bands belonged to the same emitting centers.

As can be seen in the luminescence and excitation spectra of sample 3 (Figure 2), the additional sintering at a high temperature leads to vanishing of the UV luminescence peak. The resulting luminescence spectrum of sample 3 exhibits a low intensity analogous to the luminescence spectrum of YAG : Ce single crystals or ceramics.[3–10] These changes could not be related to the oxidation of cerium since the additional thermal treatment (as well as the synthesis) was performed in a mixture of $3H_2 + N_2$. This is also confirmed by the fact that the visible luminescence intensity after additional sintering was 12% higher than that observed in sample 2 and equal to the visible luminescence intensity of sample 1.

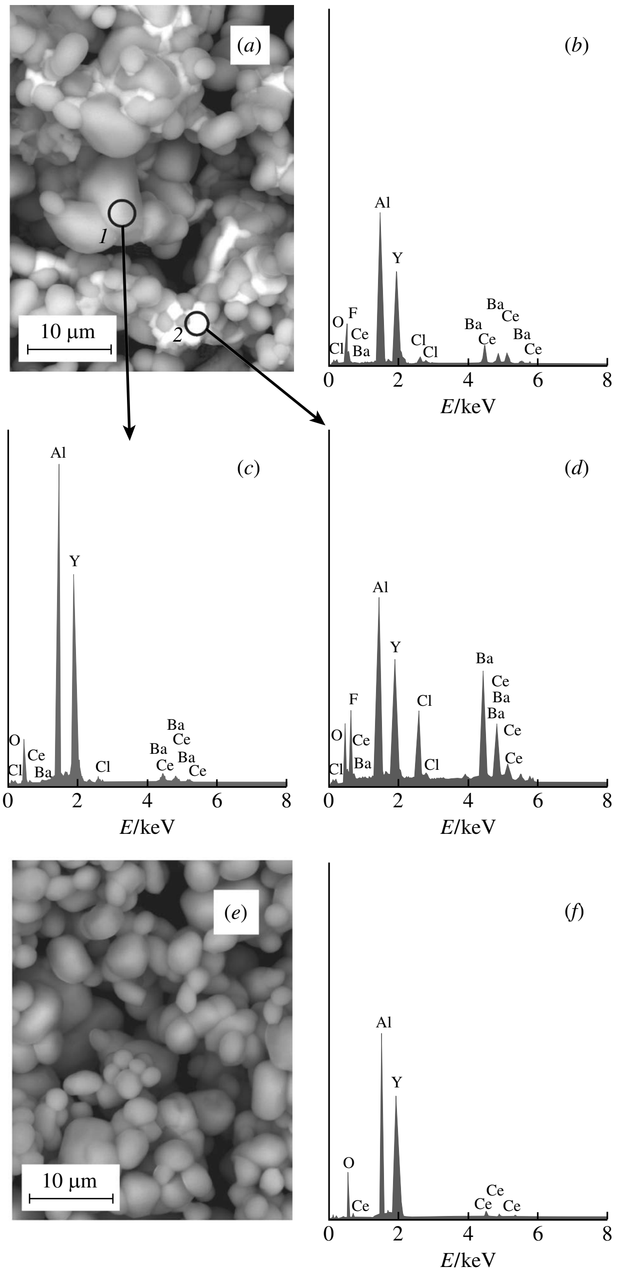

Figure 3 SEM images of (*a*) sample 2 and (*e*) sample 3 and EDAX diagrams of (*b*) sample 2, (*c*), (*d*) sample 2 at points *1* and *2*, respectively [indicated in Figure 3(*a*)], and (*f*) sample 3.

Thus, we suggested that the vanishing of UV luminescence was related to the disappearance of some impurity phases, which were formed during synthesis and evaporated when sample 3 was additionally calcined in a reductive atmosphere at high temperatures.

The SEM micrographs (Figure 3)[§] show the morphology of the YAG : Ce product with a Ce concentration of 3% synthesized at 1500 °C (sample 2) and additionally heated at 1560 °C (sample 3).

[‡] The excitation and luminescence spectra were measured at room temperature on a Varian Cary Eclipse fluorescence spectrophotometer equipped with a xenon flash lamp as the excitation source. As previously,[1] we studied the spectra of strongly diluted (0.25 wt%) suspensions of phosphor powders in glycerol. Using this approach, we minimized the light reabsorption effect and thus obtained additional information on the optical properties of phosphors.

In the first case, we can identify two different phases, namely, a garnet phase (gray spherical particles) and white formless inclusions localized between the particles of the main phase. In sample 3, white inclusions were not found.

The EDAX analysis of sample 3 [Figure 3(*f*)] allowed us to conclude that the phosphor particles contained only the Al, Y, O and Ce elements.

For sample 2 EDAX diagrams characterize compositions in two different dots. The dot *1* is located in white phase and the dot *2* is situated on the surface of main phase. According to EDAX data, the concentrations of Ba, F and Cl in dot *2* are many times higher than those in point *1*.

Thus, white alien inclusions located between garnet phase particles can be considered as a solidified melt of barium halides, which exist as a liquid phase at high temperatures. The presence of this phase, on the one hand, favors the growth of YAG : Ce crystals and, on the other, provides the formation of a phase responsible for the appearance of the ultraviolet luminescence.

In conclusion, the results of this investigation demonstrate that the high-intensity UV luminescence of commercial YAG : Ce phosphors is caused by the presence of impurity phases including barium fluoride and barium chloride. Evaporation of these phases at high temperatures in a reductive medium leads to the disappearance of UV luminescence, while the intense yellow-green emission from the YAG:Ce phosphor excited by a blue LED is retained.

This work was supported by the INCOTEX Holding, Fultor Enterprises Ltd. and Department of Physics of the M. V. Lomonosov Moscow State University. We are grateful to the Center of Collective Equipment Usage at the D. I. Mendeleev University of Chemical Technology of Russia.

References

1 A. V. Vishnyakov, E. A. Vishnyakova, Y. Chang, I. V. Ivanov and T. Yu. Kiseleva, *Tech. Phys. Lett.*, 2014, **40**, 448.

2 W. M. Yen, S. Shionoya and H. Yamamoto, *Phosphor Handbook*, 2nd edn., CRC Press/Taylor and Francis, Boca Raton, FL, 2007.

3 G. Blasse and A. Bril, *Appl. Phys. Lett.*, 1967, **11**, 53.

4 D. J. Robbins, B. Cockayne, J. L. Glasper and B. Lent, *J. Electrochem. Soc.*, 1979, **126**, 1213.

5 S. R. Rotman, H. L. Tuller and C. Warde, *J. Appl. Phys.*, 1992, **71**, 1209.

6 C. M. Wong, S. R. Rotman and C. Warde, *Appl. Phys. Lett.*, 1984, **44**, 1038.

7 E. Mihóková, M. Nikl, J. A. Mareš, A. Beitlerová, A. Vedda, K. Nejezchleb, K. Blažek and C. D'Ambrosio, *J. Lumin.*, 2007, **126**, 77.

8 V. Pankratov, L. Grigorjeva, D. Millers and T. Chudoba, *Radiation Measurements*, 2007, **42**, 679.

9 S. V. Nizhankovsky, A. Ya. Dan'ko, O. V. Zelenskaya, V. A. Tarasov, Yu. V. Zorenko, V. M. Puzikov, L. A. Grin', A. G. Trushkovskii and V. P. Savchin, *Tech. Phys. Lett.*, 2009, **35**, 964.

10 Yu. Zorenko, T. Voznyak, V. Gorbenko, E. Zych, S. Nizankovski, A. Dan'ko and V. Puzikov, *J. Lumin.*, 2011, **131**, 17.

Received: 26th November 2014; Com. 14/4514

[§] The morphology and chemical compositions of the samples were investigated on a Nova NanoSEM 230 scanning electron microscope (SEM) (FEI Company) equipped with a system of local energy-dispersive X-ray analysis (EDAX). The detection limits of the test elements were 0.5%, and the relative error of the signal amplitude was < 10%.